PLUTO'S ATMOSPHERE AND A TARGETED-OCCULTATION SEARCH FOR OTHER BOUND KBO ATMOSPHERES ⋆

J. L. ELLIOT[1,2] and S. D. KERN[1]

[1] *Department of Earth, Atmospheric, and Planetary Sciences, Massachusetts Institute of Technology (MIT), 77 Massachusetts Avenue, Cambridge, MA 02139-4307, U.S.A.;* [2] *Department of Physics, MIT; and Lowell Observatory, 1400 West Mars Hill Road, Flagstaff, AZ 86001-4499, U.S.A.*

Abstract. Processes relevant to Pluto's atmosphere are discussed, and our current knowledge is summarized, including results of two stellar occultations by Pluto that were observed in 2002. The question of whether other Kuiper belt objects (KBOs) may have bound atmospheres is considered, and observational indicators for KBO atmospheres are described. The definitive detection of a KBO atmosphere could be established with targeted stellar-occultation observations. These data can also establish accurate diameters for these objects and be used to detect possible nearby companions. Strategies for acquiring occultation data with portable, airborne, and fixed telescopes are evaluated in terms of the number of KBO occultations per year that should be observable. For the sample of 29 currently known KBOs with $H \leq 5.2$, (radius $\leq$ 300 km for a geometric albedo of 0.04), we expect about 4 events per year would yield good results for a (stationary) 6.5-m telescope. A network of portable 0.36-m telescopes should be able to observe 6 events per year, and a 2.5-m airborne telescope would have about 200 annual opportunities to observe KBO occultations.

1. Introduction

Under the influence of solar heating, cometary ice sublimates into the beautiful coma and tail that has become the hallmark of these bodies in the popular literature. Their gravity is too weak to overcome the velocity of the escaping gas and its entrapped dust. More massive bodies, however, have sufficient gravity to hold back the sublimated gas in the form of a bound atmosphere that can last for the age of the solar system. The gas lost to exospheric escape into space can be replenished from surface volatiles.

Given that bound atmospheres exist on Pluto, and Neptune's satellite Triton (an ex-KBO with a size and density similar to Pluto), it is natural to ask whether other denizens of the Kuiper belt also have bound atmospheres. Our first step toward answering this question is to lay out the physical conditions necessary for a bound atmosphere, according to our present understanding. Certainly the larger bodies – especially those with high albedo – would be the most promising candidates. Stern et al. (1988) used the high albedo of Pluto to infer that it had an atmosphere

⋆ Presented as "Pluto: The only Kuiper Belt Object with a Bound Atmosphere?" at the First Decadal Review of the Edgeworth–Kuiper Belt, Antofagasta, Chile, 11–14 March, 2003.

Earth, Moon and Planets **92:** 375–393, 2003.

prior to its direct detection by a stellar occultation in 1988 – although the observers were not aware of this inference, since it appeared in the literature well after the event (Elliot et al., 1988). Both the size and albedo contribute to the H magnitude, which may prove to be an effective observational indicator for the presence of an atmosphere. [The H magnitude is defined as the V magnitude of a body at 1 AU from both the Sun and the observer at zero phase angle (Bowell et al., 1989). The smaller the H magnitude, the larger and/or brighter is the body.]

More direct evidence for an atmosphere would be the spectral identification of bands of common ices whose sublimated gases (at the surface-ice temperature of the body) might remain gravitationally bound. This approach led Cruikshank and Silvaggio (1979) to propose that Triton had an atmosphere a decade prior to its direct detection by Voyager 2 with a radio occultation (Tyler et al., 1989). Even more definitive observations would be the detection of spectral signatures unique to the gaseous phase (as distinct from the solid phase) of CH_4, O_2, N_2 or CO. Although the latter three molecules have weak spectral bands (due to the nearly complete absence of a dipole moment), the direct detection of CH_4 gas has been achieved for Pluto by Young et al. (1997).

Tenuous atmospheres can be more easily detected with occultations – provided, of course, that suitable occultation events can be identified and successfully observed for the body of interest. These could be (i) occultations of spacecraft radio signals (e.g., Tyler et al., 1989), (ii) solar or stellar occultations observed from a flyby or orbiting spacecraft (e.g., Broadfoot et al., 1989), or (iii) stellar occultations observed from Earth (e.g., Elliot et al., 1995a; Elliot and Olkin, 1996). The latter includes observations from fixed and portable ground-based telescopes, airborne telescopes – such as the Stratospheric Observatory for Infrared Astronomy (SOFIA) – and Earth-orbiting telescopes, such as the Hubble Space Telescope (HST).

In this paper we discuss the processes that occur in Pluto's atmosphere, as an example of a bound KBO atmosphere. Then we investigate how we might search for bound KBO atmospheres with what we term "targeted" stellar occultations. By "targeted" we mean those occultations that can be predicted in advance for specific KBOs, from a knowledge of their orbits and a catalog of stars that lie near their projected paths through the sky. This type of occultation is in contrast with the occultation surveys (e.g., Alcock et al.; Roques et al., these proceedings) proposed to search for small KBOs.

Stellar occultations are a particularly sensitive probe for bound gaseous atmospheres, because of their exponential refractivity gradients. These are distinct from rapidly escaping "particulate" atmospheres – such as cometary comas – which are more easily detected by imaging observations (because of the large amount of light scattered per unit mass by small particles). For example, the coma of (2060) Chiron – suspected from the body's unusual photometric activity (Tholen et al., 1988) – was first revealed with imaging data (Meech and Belton, 1990; Luu and Jewitt, 1990). The extinction of starlight due to concentrated "jets" of material from (2060)

Chiron's nucleus (and perhaps a bound coma), however, were later detected with a stellar occultation (Elliot et al., 1995b).

2. Pluto's Atmosphere

2.1. PROCESSES

Pluto is an example of a small, icy-body whose atmosphere originates from the sublimation of surface ice. This process is illustrated in the diagram of Figure 1, where the solid horizontal line corresponds to the body's surface. Volatiles from the interior of the body can reach the surface by a variety of processes (Stern, 1989; McKinnon et al., 1997), where impinging sunlight causes sublimation. Areas of ice in shadow are cooler and will be sites of frost condensation, with the accompanying release of heat. However, the temperature difference between the shaded and sunlit ice is small, since the processes of sublimation and condensation act as a thermostat to keep the surface ice within a fraction of a degree around the body (Trafton and Stern, 1983). This process results in the net transport of frost from equatorial regions to the polar regions (Spencer et al., 1997; Hansen and Paige, 1996). This mechanism does not operate for extremely tenuous atmospheres (such as that of Io), since the flow that would be required to maintain equilibrium would be greater than the speed of sound (Ingersoll, 1990).

The gaseous inventory of an icy-body atmosphere can be established to some extent from its near-IR spectrum, which can reveal the molecular bands of certain ices (e.g., CH_4, N_2, CO), if present, while other ices (e.g., Ar) have no detectable bands in easily accessible spectral regions. If the mole fractions of the surface ices are known (either by spectroscopic evidence or other lines of reasoning), we can refer to the vapor-pressure curves of Figure 2 and use Raoult's law to deduce the partial pressures of the atmospheric constituents (e.g., Owen et al., 1993).

Photochemical processes (Summers et al., 1997; Lara et al., 1997; Krasnopolsky and Cruikshank, 1999) and dynamical processes (Ingersoll, 1990) also occur in icy-body atmospheres, and models for these have been most extensively developed for Triton, based on the information gained from the Voyager 2 flyby in 1989 (Yelle et al., 1995; Strobel and Summers, 1995). Also, the structure of small-body atmospheres in the early outer solar system has been considered by Rao (2001). For our work, however, the process of atmospheric escape will be the most important for the task of determining which bodies can retain an atmosphere.

The thermal structure of an icy-body atmosphere in the outer solar system is controlled by radiative and conductive processes. Beginning with the model of Yelle and Lunine (1989), the radiative-conductive models developed for Pluto's atmosphere have become increasingly sophisticated (Hubbard et al., 1990; Lellouch, 1994). Virtually the same models apply to Triton's atmosphere (e.g., Stevens et al., 1992), since their principal atmospheric constituents are the same, and

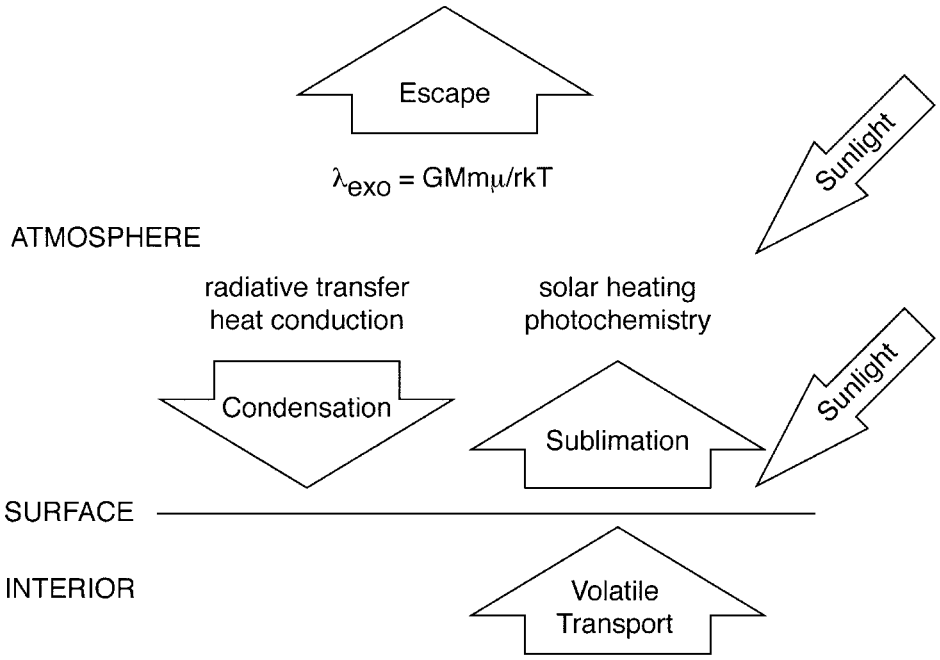

Figure 1. Processes in icy-body atmospheres. Processes for transport of volatiles to the surface include diffusion, solid-state convection, surface gardening and internal activity (Stern, 1989; McKinnon et al., 1997). The horizontal line defines the body's surface, where frost sublimates in sunlight and condenses in shadows. If the surface temperature is sufficiently high, vapor-pressure equilibrium can be maintained, which keeps the ice temperature at a nearly constant value over the entire surface. At the top of the atmosphere, the rate of escape is determined by the ratio of thermal energy to the gravitational potential (see text).

currently these bodies are at nearly equal solar distances. The most recent radiative-conductive model is that of Strobel et al. (1996), which includes heating from the 2.3- and 3.3-μm vibrational bands of CH_4, as well as cooling by the 7.6-μm vibrational band of CH_4, the rotational lines of CO, and heat conduction to the surface. The potential role of aerosols has been discussed by Lellouch (1994). From these models one can estimate the exospheric temperature, which controls atmospheric escape.

Jeans escape of gas from the top of the atmosphere occurs when a molecule, through random collisions, acquires a velocity sufficiently high to overcome the body's gravity. Hydrodynamic escape occurs when the gas escapes by flowing out of the atmosphere in bulk (e.g., Trafton et al., 1997). The escape rates for both processes are limited by the solar energy absorbed at high altitudes, and both are determined by the ratio of the thermal energy of a molecule to the gravitational potential well (Chamberlain and Hunten, 1987). If G is the gravitational constant, k is Boltzmann's constant, M is the atomic mass unit, μ is the molecular weight of

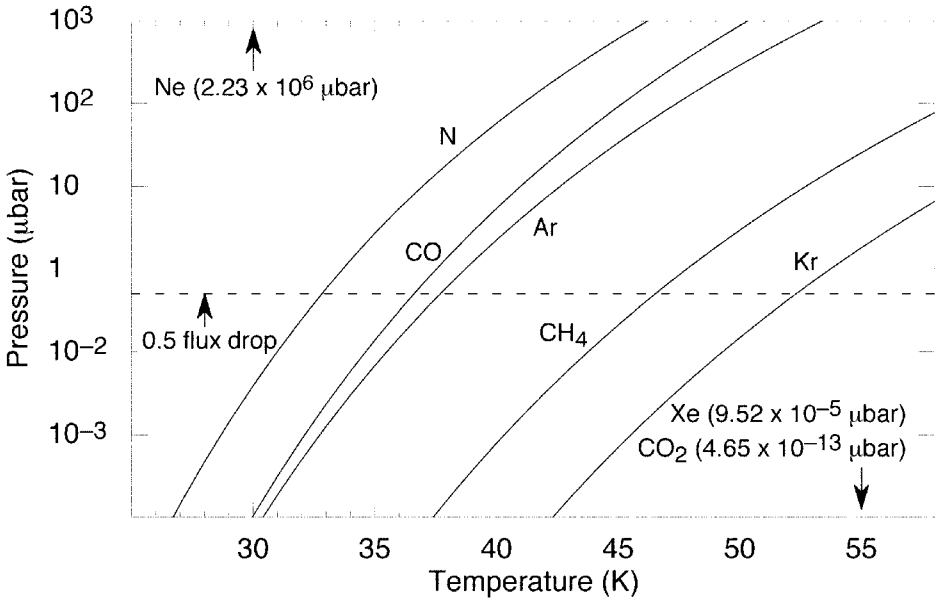

Figure 2. Vapor pressure of ices. The plot relates the temperature versus vapor pressure for five ices (N_2, CO, Ar, CH_4, Kr) that could be found within a bound atmosphere of an icy-body in the outer solar system. Volatiles Xe and CO_2 have vapor pressures much too low at these temperatures to appear in this plot, while the vapor pressure for Ne is too high (data from Brown and Ziegler, 1980). The horizontal line indicates the surface pressure for which the stellar flux would have dropped by 0.5 of its unocculted value at the surface radius for a body similar to Charon at 40 AU that has a bound N_2 atmosphere.

the gas, m is the mass of the body, r is its surface radius, and $T_{\rm exo}$ (denoted as T in Figure 1) is its exospheric temperature, then $\lambda_{\rm exo}$ is given by the equation:

$$\lambda_{\rm exo} = \frac{GM\mu m}{rkT_{\rm exo}}. \tag{1}$$

Escaping volatiles are replenished by sublimation of surface ices. For example, Trafton et al. (1997) have estimated that Pluto has lost a depth of up to 3 km of N_2 ice over the age of the solar system that has sublimated into the atmosphere and then escaped into space, while Krasnopolsky (1999) has estimated the amount to be only ∼0.5 km. Since this process depends exponentially on $\lambda_{\rm exo}$, it is much more effective on bodies less massive than Pluto. Measurement of the atmospheric escape from Pluto is one of the objectives of the New Horizons Pluto mission (Stern and Spencer, these proceedings; http://pluto.jhuapl.edu/mission.htm).

2.2. CURRENT UNDERSTANDING

The direct detection of Pluto's atmosphere was made in 1988 with a stellar occultation (Elliot et al., 1988; Hubbard et al., 1988; Elliot et al., 1989; Millis et al., 1993). For a review of the mechanics of atmospheric occultations, the reader is referred to Elliot and Olkin (1996), and for a comprehensive overview of Pluto's atmosphere prior to the 2002 stellar occultations, Yelle and Elliot (1997) should be consulted. Figure 3 reproduces a recent summary of observational constraints (Elliot et al., 2003b) on the structure of Pluto's atmosphere, which has been updated here (bold) for the 2002 stellar occultation results (Elliot et al., 2003a; Sicardy et al., 2003).

From surface-ice spectra (e.g., Owen et al., 1993) and the assumption of vapor-pressure equilibrium, it can be inferred that the atmosphere is composed predominantly of N_2, with trace amounts of CO and CH_4. Combining this knowledge with the occultation results yields a mean atmospheric temperature of 104 ± 8 K for a pure N_2 atmosphere (Elliot and Young, 1992), where the error bar has been reduced from the published value to reflect an improvement in our knowledge of Pluto's mass (Null and Owen, 1996; Foust et al., 1997; Olkin et al., 2003). A further constraint on the atmospheric structure is placed by mutual-event measurements of Pluto's surface radius (see Binzel and Hubbard, 1997 for a review). The result of Young and Binzel (1994), who included limb-darkening in their analysis, is plotted in Figure 3. Also plotted in Figure 3 is the measurement of the surface-ice temperature of 40 ± 2 K by Tryka et al. (1994), for which the error bar in radius has been calculated from the error bar in temperature under the assumption of vapor-pressure equilibrium.

An important question about Pluto's atmosphere raised by the 1988 occultation data – particularly from the Kuiper Airborne Observatory (KAO) data set – is the "kink" (a.k.a. "knee") in the occultation light curve (plotted as points in Figure 4) that has been interpreted alternatively as (i) extinction arising from a sharply bounded extinction layer (Elliot et al., 1989; Elliot and Young, 1992) or (ii) the onset of a steep thermal gradient (Eshleman, 1989; Hubbard et al., 1990). One way to distinguish between the two proposals would be a multi-wavelength occultation observation: extinction effects would cause the occultation light curve to be different at different wavelengths (due to wavelength dependent absorption by sub-micron sized particles), while a steep thermal gradient would cause very little wavelength dependence of the light curves (because refractivity is a weak function of wavelength).

To determine the cause of the kink and to investigate possible changes in Pluto's atmosphere since 1988, two stellar occultations were observed in the summer of 2002. The data set from the first occultation indicated that Pluto's atmosphere had changed (Buie et al., 2002), but the data were not of sufficient quality for further conclusions. The second occultation was more extensively observed, and these results led to several conclusions (Elliot et al., 2003a; Sicardy et al., 2003): (i) the kink in the light curve has disappeared, (ii) the atmospheric pressure within

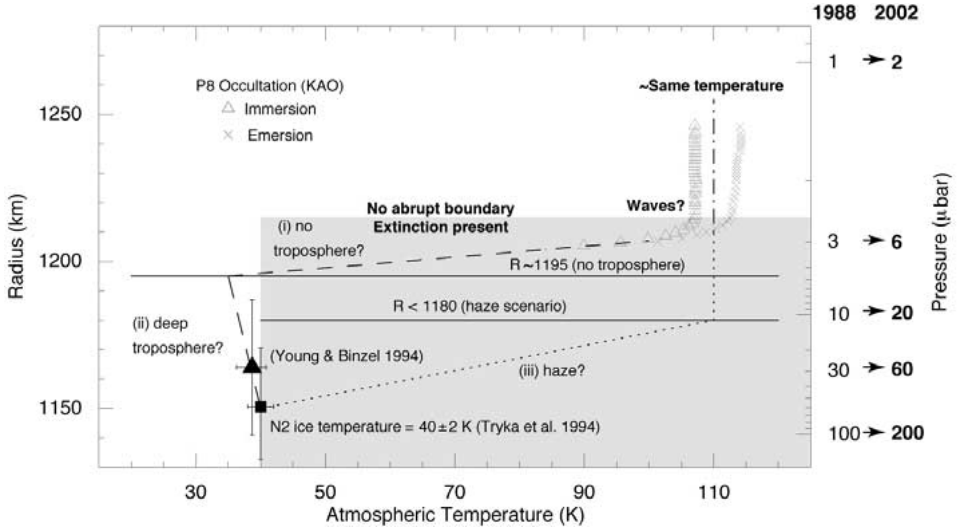

Figure 3. Possible thermal profiles for Pluto's atmosphere in 1988 with updated pressure (P) values for 2002 on the right-hand scale. Other results from the 2002 occultations are indicated in bold. Temperature is plotted versus radius for three different thermal scenarios: (i) "no troposphere", (ii) "deep troposphere", and (iii) "haze". For the first two scenarios, extinction effects in the occultation light curve are assumed to be negligible. The pressure scale on the right is based on the deep-troposphere scenario. For all scenarios a predominantly N_2 atmosphere in vapor-pressure equilibrium with surface ice is assumed. The thermal inversion results (Elliot et al., 2003b) for immersion and emersion are plotted as points (without error bars), while unmeasured parts of the profiles are plotted as lines. For the no-troposphere scenario, the thermal profile would follow the steep slope indicated by the inversion until the surface is reached ($r = 1150$ km, $P = 60$ μbar). However, if the atmosphere has a deep troposphere (Stansberry et al., 1994), the thermal profile would reach a minimum at the radius indicated by the no-troposphere scenario, but then it would continue a convective profile to the surface. The maximum temperature gradient would be the dry adiabatic gradient of $-g(r)/c_p = -0.61$ K km^{-1} (for $r = 1175$ km, where c_p is the specific heat at constant pressure for N_2), but smaller convective gradients have been discussed (Stansberry et al., 1994). In this scenario, the surface radius and pressure are not constrained and could match any value indicated by the mutual events (Young and Binzel, 1994). In the haze scenario, the steep drop in the occultation light curve is postulated to be caused by extinction effects in the atmosphere, so the temperature profile below the top of the haze layer ($r = 1225$ km, $P = 2.5$ μbar) is unconstrained, although the temperature must decrease in some manner to reach a value at the surface that would be consistent with vapor-pressure equilibrium for N_2 ice at a surface temperature of 40 ± 2 K (Tryka et al., 1994; figure adapted from Elliot et al., 2003b).

the altitude range probed by the occultation increased by a factor of two between 1988 and 2002, (iii) the temperature in this region is virtually the same for both occultations, (iv) dynamical activity in the region of Pluto's atmosphere probed in 2002 is much stronger than in the region probed in 1988, and (v) an asymmetry in Pluto's atmospheric structure is observed. Furthermore, the multi-wavelength observations show a wavelength dependence in the minimum flux of the occultation light curve (Elliot et al., 2003a). This wavelength dependence can be interpreted

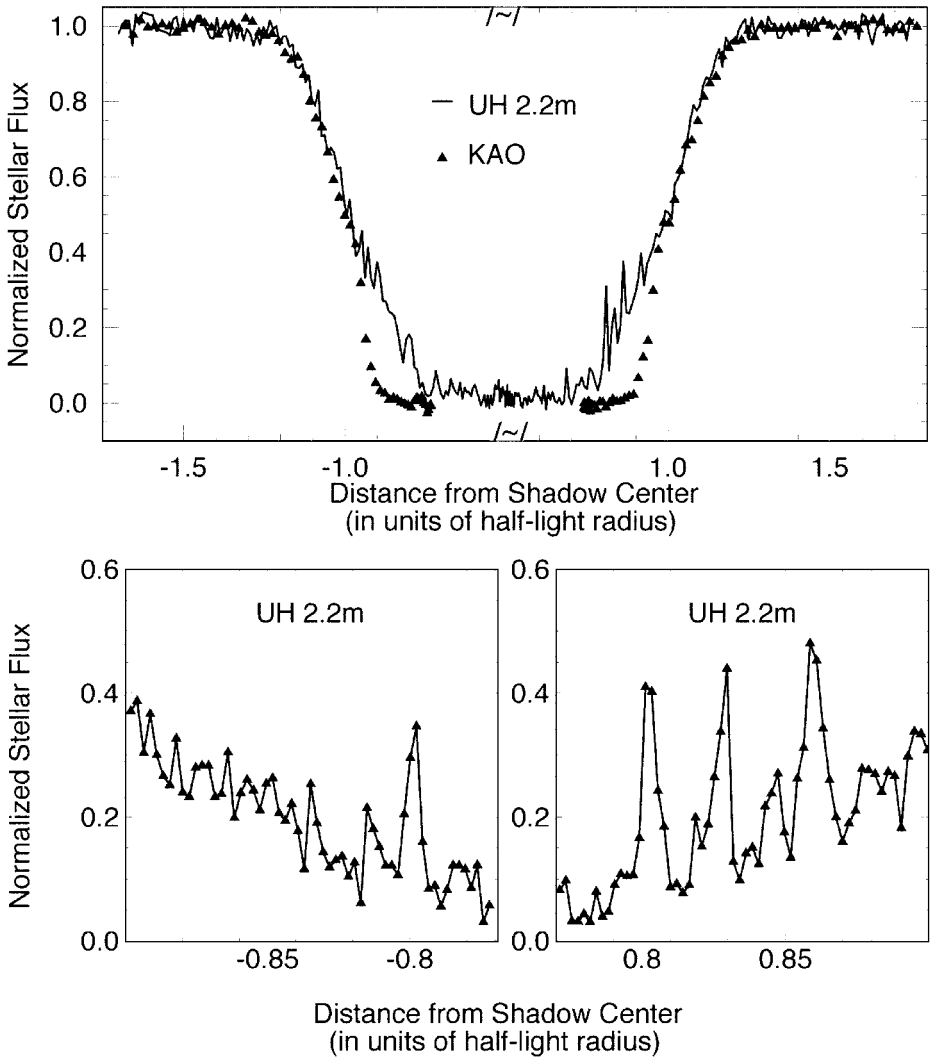

Figure 4. Pluto occultation light curves. The KAO data from the June 9, 1988 event (triangles), and the UH 2.2-m data from the August 21, 2002 event (line) have been plotted versus distance from the center of their occultation shadows. The distance scale has been normalized in units of half-light radius. The "spikes" (short flashes of starlight, Elliot and Veverka, 1976) in the UH 2.2-m data are seen in the blow-up below the comparison figure. These will be discussed in a later publication. Note that the 1988 light curve drops sharply to zero just below half light, whereas the 2002 light curve has no such "kink" (after Elliot et al., 2003a).

as due to extinction effects in Pluto's atmosphere, although the presence of a faint, red companion to the occulted star could have caused the same effect. This latter possibility can be tested with high-resolution imaging of the occulted star.

3. What KBOs Might Have Bound Atmospheres?

3.1. Requirements for a small-body atmosphere

For a small body to have a bound atmosphere, three conditions must be satisfied. First, the body must have an inventory of volatiles on its surface that can sublimate (e.g., N_2, CO, CH_4); second, the temperature must lie within the correct range – high enough for adequate vapor pressure (Figure 2), but not so high that the atmosphere would escape into space; and third, the body's mass must be sufficient to retain the atmosphere. These three factors can be considered together in the escape parameter, $\lambda_{\rm exo}$, as defined by Equation (1). The escape parameter is calculated with the exospheric temperature, $T_{\rm exo}$. For incipient atmospheres, however, we expect the exospheric temperature to be very close to the equilibrium blackbody temperature of the surface ice. To be explicit for this situation, we denote the escape parameter by $\lambda_{\rm surf}$. We assume a spherical body of radius r, density ρ, geometric albedo p, and phase integral q ($\sim$0.5 for the icy Uranian satellites, Helfenstein et al., 1988). The body has a surface volatile of molecular weight μ and is at a solar distance D. If this body is of uniform temperature, i.e., its surface temperature is determined by radiative equilibrium with solar radiation, then the escape parameter is given as $\lambda_{\rm surf}$ by Equation (2), which has been normalized to parameters approximately appropriate for Charon at 40 AU:

$$\lambda_{\rm surf} = 14\left[\frac{0.8}{(1-0.5p)}\right]^{\frac{1}{4}}\left[\frac{\mu}{28}\right]\left[\frac{\rho}{1.7\,{\rm g\,cm^{-3}}}\right]\left[\frac{r}{625\,{\rm km}}\right]^2\left[\frac{D}{40\,{\rm AU}}\right]^{1/2}. \qquad (2)$$

In Figure 5 we have used Equation (2) to calculate contours for constant values of $\lambda_{\rm surf}$ in the body-radius vs. solar-distance plane with all other parameters fixed at their normalizing values. Horizontal lines are plotted for an icy body of radius 1175-km, Charon, and Quaoar. Charon and Quaoar have nearly the same radii, but Charon covers a much greater range of solar distances. Not plotted in Figure 5 is the region, at large solar distances, where vapor-pressure equilibrium would break down, when (as the surface becomes colder and the atmosphere becomes more tenuous due to the drop in the surface pressure) the required flow velocity becomes comparable to the sonic velocity (Ingersoll, 1990).

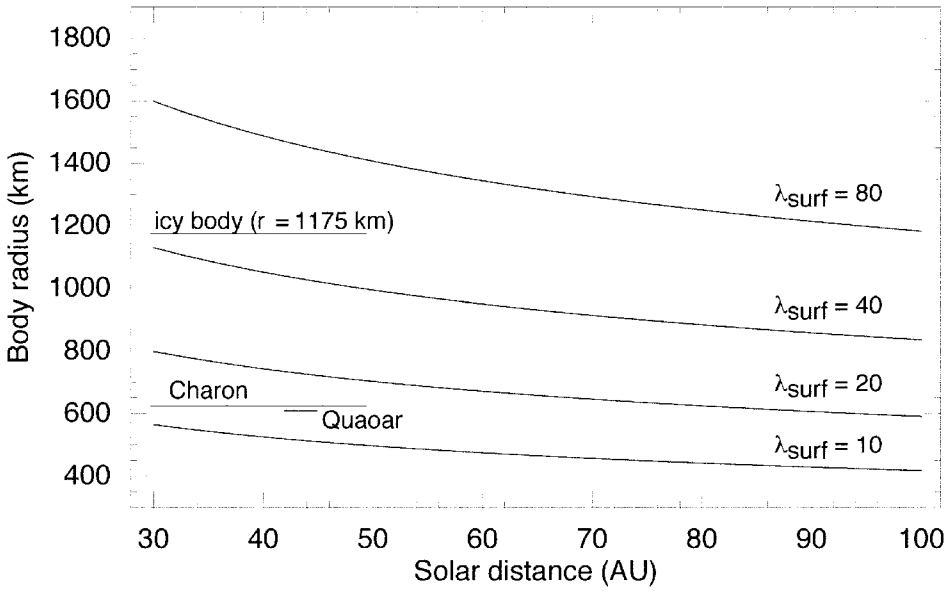

Figure 5. Contours for the atmospheric escape parameter plotted in the body-radius vs. solar-distance plane. This plot shows lines for constant λ_{surf} as given by Equation (2). The calculation applies to an ideal slowly rotating black body with N_2 surface ice and the albedo of Charon (see text). Horizontal lines for an icy body of radius 1175 km, Charon, and Quaoar cover a range of solar distances for comparison.

3.2. H-MAGNITUDE: AN ATMOSPHERIC INDICATOR?

The most likely KBO candidates for atmospheres are those that reflect the most light because they have the largest radii and/or highest albedos (perhaps indicative of freshly condensed frost). This can be quantified by the H magnitude of the body and is illustrated in Figure 6, where we have plotted the radius versus H magnitude for Pluto, Triton, Charon, and a selection of KBOs. The radii of Varuna and Quaoar are plotted at the values measured with the radiometric technique, and the radii for the others are plotted for assumed geometric albedos of 0.04 and 0.64. Pluto and Triton, with known N_2 atmospheres, lie to the far right of the plot. Just to their left is Charon, and to its left lie the other currently known KBOs. We see that the main KBO population lies well above Charon in H magnitude – because Charon has a somewhat higher albedo than yet measured for any KBO other than Pluto. It should be noted, however, that Charon's albedo is significantly less than several icy Saturnian satellites that (presumably) have no atmospheres.

3.3. DOES CHARON HAVE AN ATMOSPHERE?

The anomalously high albedo of Charon compared with the handful of KBOs for which we have measured albedos leads one to wonder whether it might have an

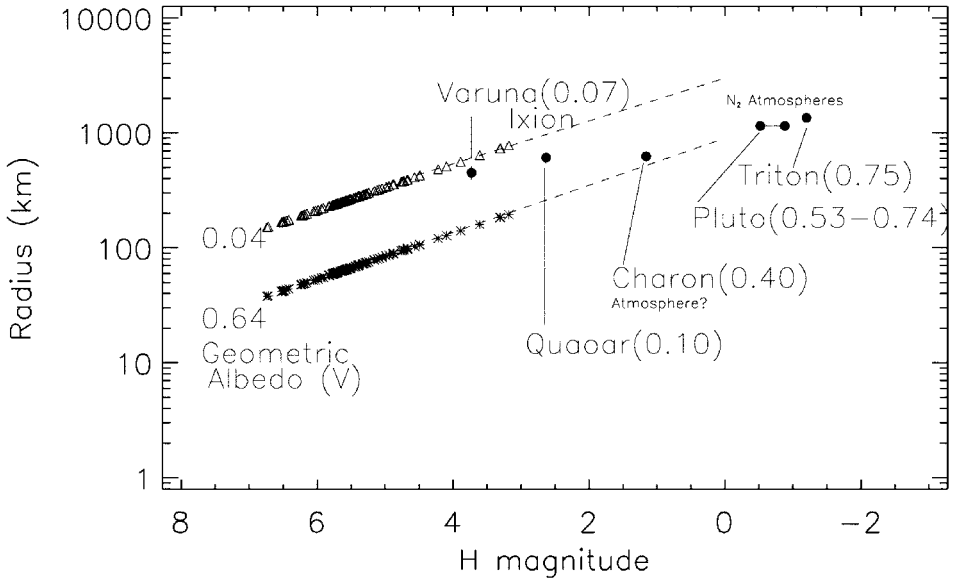

Figure 6. H-magnitude an atmospheric indicator? The H-magnitudes for the brightest KBOs are plotted versus radius. The solid circles are actual measurements for individual KBOs while the triangles and stars represent the current population of bright objects if their albedos were determined to be 0.04 and 0.64 respectively. Pluto and Triton have substantially high albedos and also have atmospheres. Charon's albedo is somewhat lower, but significantly greater than that for Quaoar, Ixion and smaller KBOs. Occultation measurements on a number of bright objects will allow us to constrain KBO radii and likewise tell us something about the general albedo trend of these objects.

atmosphere. A stellar occultation was observed by Walker (1980), who determined a lower limit on the radius of Charon from his single-chord observation. The data show no obvious evidence for an atmosphere, although the time resolution is low (2.0 s). These data were analyzed further by Elliot and Young (1991), who found that the immersion and emersion events differed from those expected from an atmosphere-less body at the 2-σ level. In their Figure 2 we see that for both the immersion and emersion events, the light-curve point adjacent to the main drop is slightly lower than the full-scale signal from the unocculted star. No firm conclusions can be drawn from this result, but we recommend that additional Charon occultation data be obtained with adequate signal-to-noise and time resolution to probe for an atmosphere.

4. Targeted KBO Occultations

Direct detection of potential KBO atmospheres can be done with stellar occultations, but to achieve this objective, one must identify events that can be observed with sufficiently high signal-to-noise. Successful occultation observations will al-

low us not only to probe for atmospheres, but these data could reveal nearby companions to the primary body. Also, they provide a direct measurement of the diameter of the KBO. This goal requires either (i) occultation light curves for the same event at different sites, or (ii) the combination of a single occultation light curve with an accurate measurement of the minimum angular separation between the KBO and the occulted star (Olkin et al., 1996). The latter approach is based on the assumption of a spherical occulting body.

In setting up a program of targeted KBO occultations, we can benefit from the experience gained in the observation of occultations by Pluto, Charon, Triton, and Chiron. The challenges for these occultations have been twofold: (i) generating an accurate prediction for the location of the occultation path on Earth, and (ii) observing these events with a telescope large enough to obtain a light curve with adequate signal-to-noise. Consider the prediction problem. In Table I these four bodies are listed, along with information relevant for occultation work. In particular, column 5 gives the present angular radius, which determines the astrometric accuracy required for the prediction. The next column gives the number of occultations that have been successfully observed. We note that two events have been observed for Chiron – whose radius subtends an angle of only 0.014 arcsec. This bodes well for a KBO occultation program, since the largest of these bodies subtend comparable angles. The difficulties for generating reliable predictions of these events are several fold. For Pluto, Charon, and Triton, the main difficulty is carrying out accurate astrometry in the proximity of another body. Prediction astrometry for most KBOs and Centaurs does not have this problem, but is hindered by a lack of faint astrometric standards. Furthermore, their ephemerides will require considerable refinement.

Figure 7 illustrates the path of the P126A occultation by Pluto that occurred on July 20, 2002. The three straight lines across northern South America represent the northern limit, center line, and southern limit of Pluto's shadow for a 10% drop in stellar flux. The positions of several observatories are indicated, but they were outside of Pluto's shadow and did not record the event. For a KBO occultation the path would be 0.1–0.5 the size of the Pluto path, which – if well placed – could be observed by two of the large-telescope facilities indicated on the diagram.

Meeting the challenge of achieving adequate signal-to-noise for an occultation can be accomplished with the observation of either (i) a bright-star event with a small telescope, or (ii) a faint-star event with a large telescope. Although bright-star opportunities occur less frequently, the mobility of small telescopes has allowed that approach to be a viable strategy for occultation work in the past. Fixed telescopes and the KAO have also been used to observe occultations. A combination of these strategies has provided the most valuable data sets. In Table II we compare these three strategies in terms of their respective rates of opportunities for the observation of KBO occultations. The first column gives the size of the telescope employed by each strategy, which sets the limiting R magnitude (next column) for the occulted star that would give a signal-to-noise ratio of 10 for a 1-second

TABLE I
Targets for occultations

Body	Mag (R)	D[a] (AU)	Radius[b] (km)	Radius[b] (arcsec)	Occ. obs.
Triton	13.4	30.1	1438 ± 17[c]	0.067	5
Pluto	14.0	30.6	1214 ± 20[d]	0.055	4
Charon	16.0	30.6	621 ± 21[e]	0.028	1
(2060) Chiron	17.1	12.1	90 ± 7[f]	0.010	2
(5145) Pholus	19.2	17.9	95 ± 13[f]	0.007	0
(10199) Chariklo	17.5	13.1	137 ± 15[f]	0.014	0
(20000) Varuna	19.8	43.2	450 ± 65[g]	0.014	0
(28978) Ixion	19.1	42.9	~ 600	0.019	0
(50000) Quaoar	18.6	43.4	610 ± 65[h]	0.019	0
Canonical KBO	20.5	40.0	300	0.010	0

[a] Heliocentric distance as of 21 May 2003.
[b] Surface radius for atmosphere-less bodies; half-light radius for Pluto and Triton.
[c] Elliot et al. (2000).
[d] Elliot et al. (2003a).
[e] Olkin et al. (2003).
[f] Altenhoff et al. (2001).
[g] Jewitt et al. (2001).
[h] Trujillo, personal communication.

Figure 7. Shadow path for the P126A occultation by Pluto. The northern and southern limits for a 10% drop in stellar flux have been plotted, along with the center line, and the relative locations of the VLT, Magellan, and Gemini South are indicated for comparison. The shadow path for an occultation by Quaoar would have about half this width.

TABLE II
Strategies for targeted KBO occultation observations

Telescope strategy (aperture, m)	Limiting stellar R Mag[a]	Events per year per KBO, γ_R	Location factor, f_l	Weather factor, f_w	Combined factor, ϵ	Observable events per year,[b] $N_{\rm obs}$
Portable (0.36)	16.2	1	0.17	0.75	0.13	~6
Airborne (2.5)	18.4	12	0.58	0.95	0.55	~200
Fixed (6.5)	19.3	30	0.0067	0.60	0.0040	~4

[a]Based on SNR = 10 for a 1 second integration for the source-limited case (Dunham et al., 2000 and http://sofia.arc.nasa.gov/Science/instruments/performance/HIPO/sensitivity.html). This assumption will be valid when the sum of the read-noise for the pixels within the image, the occulting KBO and background sky light is less than the photon noise from the occulted star.
[b]For a single telescope and the current sample of 29 KBOs brighter than an H magnitude of 5.2.

integration. In the third column we give the average rate, γ_R, of occultations of stars brighter than the limiting magnitude that would occur somewhere on Earth for a canonical KBO with a 300 km radius ($H = 5.2$, for $p_V = 0.04$, as used by the Minor Planet Center) that orbits the Sun in a circular orbit at a distance of 40 AU. The next two columns present the factors that limit the number of events that can be successfully observed, and we consider these in turn.

The first, the location factor, f_l, is the fraction of the events occurring somewhere on Earth for which the occultation path passes over the telescope and the event is observable accounting for the fraction of the time that the KBO is above 20° altitude, without significant interference from sunlight and moonlight. For the airborne and portable-telescope strategies, the estimates of the location factor are based on a sample of predicted Chiron occultation paths (Bus et al., 1994; Person et al., 1996) that could have been accessible to each strategy. Portable and airborne telescopes can use their mobility to avoid the Sun and Moon, while a fixed telescope cannot. The next column contains the weather factor, f_w, which is an estimate for the fraction of events that could not be observed during cloudy conditions. We combine these into an overall factor, $\epsilon = f_1 f_w$.

In the final column we give the number of observable events per year (per telescope) with each strategy, $N_{\rm obs}$, which is given by:

$$N_{\rm obs} = \epsilon \gamma_{\rm R} N_{\rm KBO}$$

where $N_{\rm KBO}$ is the number of KBOs in the occultation program. At the time of the conference, 29 KBOs with $H \leq 5.2$ with astrometric errors less than 300 arcsec were available for such a project. This number will increase with time as new discoveries are made (Buie et al., Trujillo et al., these proceedings). However, virtually all of the KBOs included in a targeted occultation program will require additional observations to reduce the errors in their ephemerides.

The basic tasks to secure KBO occultation data include: (1) establishing a pool of KBOs for potential occultations, (2) refining the ephemerides for these KBOs, (3) establishing a list of candidate stars for each KBO, (4) prediction of the occultations, (5) requests for telescope time, (6) refinement of the predictions close to the time of the events, and (7) observation of the occultations. This work will require the use of a variety of telescopes and a cooperative effort from the KBO community.

5. Summary and Conclusions

We have discussed the atmosphere of Pluto, and used it as a basis for speculating on the possibilities for atmospheres on large KBOs. Pluto and Triton both have atmospheres of primarily N_2 in a state of vapor-pressure equilibrium. They have high albedos and have about twice the diameter of other currently known KBOs. In size, Charon is rivaled by the population of large KBOs, but it has a much higher albedo than any currently measured values for these bodies – with perhaps hints of a tenuous atmosphere revealed in occultation data from 1980 (Elliot and Young, 1991). Given the temperatures in the Kuiper Belt, one might expect to find atmospheres of N_2, CO, CH_4, Ar, or Kr (if these noble gases have been retained by KBOs in adequate abundance). Having a bound atmosphere, of course, requires that the KBO have an inventory of surface volatiles that can sublimate, that it have an appropriate temperature and lastly, that its mass is sufficient to retain an atmosphere.

Such atmospheres could be detected with targeted stellar occultations. These data will also give direct diameter measurements for these objects as well as search for close companions. This project is observationally challenging because the occultation path of a KBO on the Earth is small. An occultation prediction will require accurate astrometry of the candidate stars and much better ephemerides for the KBOs. KBO occultations could be observed with a network of portable telescopes, an airborne telescope (SOFIA), or with fixed telescopes. Each of these approaches is likely to be successful in the future, as they have been in the past for Pluto, Charon, Triton, and Chiron.

Acknowledgments

We thank M. J. Person for his comments on the manuscript and K. B. Clancy for her assistance with the graphics. Alan Stern's referee comments helped improve the paper, for which we are grateful. Partial support for this work was provided by NSF grant AST-0073447, by NASA grant NAG5-10444 and NASA-Ames grant NAS2-97001 (under subcontract from Lowell Observatory).

References

Altenhoff, W. J., Menten, K. M., and Bertoldi, F.: 2001, 'Size Determination of the Centaur Chariklo from Millimeter-Wavelength Bolometer Observations', *Astron. & Astrophys.* **366**, L9–L12.

Binzel, R. P. and Hubbard, W. B.: 1997, 'Mutual Events and Stellar Occultations', in S. A. Stern and D. J. Tholen (eds.), *Pluto*, University of Arizona Press, Tucson, pp. 85–102.

Bowell, E., Hapke, B., Domingue, D., Lumme, K., Peltoniemi, J., and Harris, A. W.: 1989, 'Application of Photometric Models to Asteroids', in R. P. Binzel, T. Gehrels, and M. S. Matthews (eds.), *Asteroids II*, University of Arizona Press, Tucson, pp. 524–556.

Broadfoot, A. L., Atreya, S. K., Bertaux, J. L., Blamont, J. E., Dessler, A. J., Donahue, T. M., Forrester, W. T., Hall, D. T., Herbert, F., Holberg, J. B., Hunten, D. M., Krasnopolsky, V. A., Linick, S., Lunine, J. I., McConnell, J. C., Moos, H. W., Sandel, B. R., Schneider, N. M., Shemansky, D. E., Smith, G. R., Strobel, D. F., and Yelle, R. V.: 1989, 'Ultraviolet Spectrometer Observations of Neptune and Triton', *Science* **246**, 1459–1466.

Brown, G. N., Jr. and Ziegler, W. T.: 1980, 'Vapor Pressure and Heats of Vaporization and Sublimation of Liquids and Solids of Interest in Cryogenics below 1-atm Pressure', *Adv. Cryog. Eng.* **25**, 662–670.

Buie, M. W., Elliot, J. L., Kidger, M. R., Bosh, A. S., Saá, O., Van Malderen, R., Uytterhoeven, K., Davignon, G., Dunham, E. W., Olkin, C. B., Taylor, B. W., Wasserman, L. H., Clancy, K., Person, M. J., Levine, S. E., Stone, R. C., Peréz-González, P. G., Pasachoff, J. M., Souza, S. P., Ticehurst, D. R., and Fitzsimmons, A.: 2002, 'Changes in Pluto's Atmosphere Revealed by the P126A Occultation', *Bull. Amer. Astron. Soc.* **34**, 877.

Bus, S. J., Wasserman, L. H., and Elliot, J. L.: 1994, 'Chiron Stellar Occultation Candidates: 1993–1996', *Astron. J.* **107**, 1814–1824.

Chamberlain, J. W. and Hunten, D. M.: 1987, *Theory of Planetary Atmospheres*, Academic Press Inc., Orlando.

Cruikshank, D. P. and Silvaggio, P. M.: 1979, 'Triton: A Satellite with an Atmosphere', *Astrophys. J.* **233**, 1016–1020.

Dunham, E. W., Elliot, J. L., and Taylor, B. W.: 2000, 'HOPI – A High-Speed Occultation Photometer and Imager for SOFIA', *Proc. S.P.I.E.* **4014**, 76–84.

Elliot, J. L. and Olkin, C. B.: 1996, 'Probing Planetary Atmospheres with Stellar Occultations', in G. W. Wetherill, A. L. Albee, and K. C. Burke (eds.), *Annual Review of Earth and Planetary Sciences*, Annual Reviews Inc., Palo Alto, pp. 89–123.

Elliot, J. L. and Veverka, J.: 1976, 'Stellar Occultation Spikes as Probes of Atmospheric Structure and Composition', *Icarus* **27**, 359–386.

Elliot, J. L. and Young, L. A.: 1991, 'Limits on the Radius and a Possible Atmosphere of Charon from its 1980 Stellar Occultation', *Icarus* **89**, 244–254.

Elliot, J. L. and Young, L. A.: 1992, 'Analysis of Stellar Occultation Data for Planetary Atmospheres. I. Model Fitting, with Application to Pluto', *Astron. J.* **103**, 991–1015.

Elliot, J. L., Dunham, E. W., and Millis, R. L.: 1988, 'Occultation by Pluto', *International Astronomical Union Circulars*, No. 4611.

Elliot, J. L., Dunham, E. W., Bosh, A. S., Slivan, S. M., Young, L. A., Wasserman, L. H., and Millis, R. L.: 1989, 'Pluto's Atmosphere', *Icarus* **77**, 148–170.

Elliot, J. L., Dunham, E. W., and Olkin, C. B.: 1995a, 'Exploring Small Bodies in the Outer Solar System with Stellar Occultations', in M. R. Haas, J. A. Davidson, and E. F. Erickson (eds.), *Proceedings of the Airborne Astronomy Symposium on the Galactic Ecosystem: From Gas to Stars to Dust*, ASP, San Francisco, pp. 285–296.

Elliot, J. L., Olkin, C. B., Dunham, E. W., Ford, C. H., Gilmore, D. K., Kurtz, D., Lazzaro, D., Rank, D. M., Temi, P., Bandyopadhyay, R. M., Barroso, J., Barucci, A., Bosh, A. S., Buie, M. W., Bus, S. J., Dahn, C. C., Foryta, D. W., Hubbard, W. B., Lopes, D. F., Marcialis, R. L., McDonald, S.

W., Millis, R. L., Reitsema, H., Schleicher, D. G., Sicardy, B., Stone, R. P. S., and Wasserman, L. H.: 1995b, 'Jet-Like Features near the Nucleus of 2060 Chiron', *Nature* **373**, 46–49.

Elliot, J. L., Person, M. J., McDonald, S. W., Buie, M. W., Dunham, E. W., Millis, R. L., Nye, R. A., Olkin, C. B., Wasserman, L. H., Young, L. A., Hubbard, W. B., Hill, R., Reitsema, H. J., Pasachoff, J. M., McConnochie, T. H., Babcock, B. A., Stone, R. C., and Francis, P.: 2000, 'The Prediction and Observation of the 1997 July 18 Stellar Occultation by Triton: More Evidence for Distortion and Increasing Pressure in Triton's Atmosphere', *Icarus* **148**, 347–369.

Elliot, J. L., Ates, A., Babcock, B. A., Bosh, A. S., Buie, M. W., Clancy, K. B., Dunham, E. W., Eikenberry, S. S., Hall, D. T., Kern, S. D., Leggett, S. K., Levine, S. E., Moon, D.-S., Olkin, C. B., Osip, D. J., Pasachoff, J. M., Penprase, B. E., Person, M. J., Qu, S., Rayner, J. T., Roberts Jr., L. C., Salyk, C. V., Souza, S. P., Stone, R. C., Taylor, B. W., Tholen, D. J., Thomas-Osip, J. E., Ticehurst, D. R., and Wasserman, L. H.: 2003a, 'The Recent Expansion of Pluto's Atmosphere', *Nature* (in press).

Elliot, J. L., Person, M. J., and Qu, S.: 2003b, 'Analysis of Stellar Occultation Data. II. Inversion, with Application to Pluto and Triton', *Astron. J.* **126**, 1041–1079.

Eshleman, V. R.: 1989, 'Pluto's Atmosphere: Models Based on Refraction, Inversion, and Vapor-Pressure Equilibrium', *Icarus* **80**, 439–443.

Foust, J. A., Elliot, J. L., Olkin, C. B., McDonald, S. W., Dunham, E. W., Stone, R. P. S., McDonald, J. S., and Stone, R. C.: 1997, 'Determination of the Charon–Pluto Mass Ratio from Center-of-Light Astrometry', *Icarus* **126**, 362–372.

Hansen, C. J. and Paige, D. A.: 1996, 'Seasonal Nitrogen Cycles on Pluto', *Icarus* **120**, 247–265.

Helfenstein, P., Veverka, J., and Thomas, P. C.: 1988, 'Uranus Satellites: Hapke Parameters from Voyager Disk-Integrated Photometry', *Icarus* **74**, 231–239.

Hubbard, W. B., Hunten, D. M., Dieters, S. W., Hill, K. M., and Watson, R. D.: 1988, 'Occultation Evidence for an Atmosphere on Pluto', *Nature* **336**, 452–454.

Hubbard, W. B., Yelle, R. V., and Lunine, J. I.: 1990, 'Nonisothermal Pluto Atmosphere Models', *Icarus* **84**, 1–11.

Ingersoll, A. P.: 1990, 'Dynamics of Triton's Atmosphere', *Nature* **344**, 315–317.

Jewitt, D., Aussel, H., and Evans, A.: 2001, 'The Size and Albedo of the Kuiper Belt Object (20000) Varuna', *Nature* **411**, 446–447.

Krasnopolsky, V. A.: 1999, 'Hydrodynamic Flow of N_2 from Pluto', *J. Geophys. Res.* **104**, 5955–5962.

Krasnopolsky, V. A., and Cruikshank, D. P.: 1999, 'Photochemistry of Pluto's Atmosphere and Ionosphere near Perihelion', *J. Geophys. Res.* **104**, 21979–21996.

Lara, L. M., Ip, W. H., and Rodrigo, R.: 1997, 'Photochemical Models of Pluto's Atmosphere', *Icarus* **130**, 16–35.

Lellouch, E.: 1994, 'Pluto's Atmospheric Structure: Clear vs Hazy Models', *Icarus* **108**, 255–264.

Luu, J. X. and Jewitt, D. C.: 1990, 'Cometary Activity in 2060 Chiron', *Astron. J.* **100**, 913–932.

McKinnon, W. B., Simonelli, D. P., and Schubert, G.: 1997, 'Composition, Internal Structure, and Thermal Evolution of Pluto and Charon', in S. A. Stern and D. J. Tholen (eds.), *Pluto and Charon*, University of Arizona Press, Tucson, pp. 295–343.

Meech, K. J. and Belton, M. J. S.: 1990, 'The Atmosphere of 2060 Chiron', *Astron. J.* **100**, 1323–1338.

Millis, R. L., Wasserman, L. H., Franz, O. G., Nye, R. A., Elliot, J. L., Dunham, E. W., Bosh, A. S., Young, L. A., Slivan, S. M., Gilmore, A. C., Kilmartin, P. M., Allan, W. H., Watson, R. D., Dieters, S. W., Hill, K. M., Giles, A. B., Blow, G., Priestly, J., Kissling, W. M., Walker, W. S. G., Marino, B. F., Dix, D. G., Page, A. A., Ross, J. E., Avey, H. P., Hickey, D., Kennedy, H. D., Mottram, K. A., Moyland, G., Murphy, T., Dahn, C. C., and Klemola, A. R.: 1993, 'Pluto's Radius and Atmosphere: Results from the Entire 9 June 1988 Occultation Data Set', *Icarus* **105**, 282–297.

Null, G. W. and Owen, W. M. J.: 1996, 'Charon/Pluto Mass Ratio Obtained with HST CCD Observations in 1991 and 1993', *Astron. J.* **111**, 1368–1381.

Olkin, C. B., Elliot, J. L., Bus, S. J., McDonald, S. W., and Dahn, C. C.: 1996, 'Astrometry of Single-Chord Occultations: Application to the 1993 Triton Event', *Publ. Astron. Soc. Pacific* **108**, 202–210.

Olkin, C. B., Wasserman, L. H., and Franz, O. G.: 2003, 'The Mass Ratio of Charon to Pluto from Hubble Space Telescope Astrometry with Fine Guidance Sensors', *Icarus* **164**, 254–259.

Owen, T. C., Roush, T. L., Cruikshank, D. P., Elliot, J. L., Young, L. A., de Bergh, C., Schmitt, B., Geballe, T. R., Brown, R. H., and Bartholomew, M. J.: 1993, 'Surface Ices and the Atmospheric Composition of Pluto', *Science* **261**, 745–748.

Person, M. J., Bus, S. J., Wasserman, L. H., and Elliot, J. L.: 1996, 'Chiron Stellar Occultation Candidates: 1996–2000', *Astron. J.* **112**, 1683–1689.

Rao, A. M. N.: 2001, *Titan, Triton, Pluto, and Kuiper Belt Objects: A Study of Past and Present Atmospheres with Grey and Non-Grey Models*, Ph.D. thesis, Department of Mathematics, University of Arizona, Tucson.

Sicardy, B., Widemann, T., Lellouch, E., Veillet, C., Cuillandre, J.-C., Colas, F., Roques, F., Beisker, W., Kretlow, M., Lagrange, A.-M., Gendron, E., Lacombe, F., Lecacheux, J., Birnbaum, C., Fienga, A., Leyrat, C., Maury, A., Raynaud, E., Renner, S., Schultheis, M., Brooks, K., Delsanti, A., Hainaut, O. R., Gilmozzi, R., Lidman, C., Spyromilio, J., Rapaport, M., Rosenzweig, P., Naranjo, O., Porras, L., Díaz, F., Calderón, H., Carrillo, S., Carvajal, A., Recalde, E., Gaviria Cavero, L., Montalvo, C., Barria, D., Campos, R., Duffard, R., and Levato, H.: 2003, 'Drastic Changes in Pluto's Atmosphere Revealed by Stellar Occultations', *Nature* **424**, 168–170.

Spencer, J. R., Stansberry, J. A., Trafton, L. M., Young, E. F., Binzel, R. P., and Croft, S. K.: 1997, 'Volatile Transport, Seasonal Cycles, and Atmospheric Dynamics on Pluto', in S. A. Stern and D. J. Tholen (eds.), *Pluto and Charon*, University of Arizona Press, Tucson, pp. 435–473.

Stansberry, J. A., Lunine, J. I., Hubbard, W. B., Yelle, R. V., and Hunten, D. M.: 1994, 'Mirages and the Nature of Pluto's Atmosphere', *Icarus* **111**, 503–513.

Stern, S. A.: 1989, 'Pluto: Comments on Crustal Composition, Evidence for Global Differentiation', *Icarus* **81**, 14–23.

Stern, S. A., Trafton, L. M., and Gladstone, G. R.: 1988, 'Why is Pluto Bright? Implications of the Albedo and Lightcurve Behavior of Pluto', *Icarus* **75**, 485–498.

Stevens, M. H., Strobel, D. F., Summers, M. E., and Yelle, R. V.: 1992, 'On the Thermal Structure of Triton's Thermosphere', *Geophys. Res. Lett.* **19**, 669–672.

Strobel, D. F. and Summers, M. E.: 1995, 'Triton's Upper Atmosphere and Ionosphere', in D. P. Cruikshank (ed.), *Neptune and Triton*, University of Arizona Press, Tucson, pp. 1107–1148.

Strobel, D. F., Zhu, X., Summers, M. E., and Stevens, M. H.: 1996, 'On the Vertical Thermal Structure of Pluto's Atmosphere', *Icarus* **120**, 266–289.

Summers, M. E., Strobel, D. F., and Gladstone, G. R.: 1997, 'Chemical Models of Pluto's Atmosphere', in S. A. Stern and D. J. Tholen (eds.), *Pluto and Charon*, University of Arizona Press, Tucson, pp. 391–434.

Tholen, D. J., Hartmann, W. K., and Cruikshank, D. P.: 1988, '(2060) Chiron', *International Astronomical Union Circulars*, 4554.

Trafton, L. and Stern, S. A.: 1983, 'On the Global Distribution of Pluto's Atmosphere', *Astrophys. J.* **267**, 872–881.

Trafton, L. M., Hunten, D. M., Zahnle, K. J., and McNutt, R. L.: 1997, 'Escape Processes at Pluto and Charon', in S. A. Stern and D. J. Tholen (eds.), *Pluto and Charon*, University of Arizona Press, Tucson, pp. 475–522.

Tryka, K. M., Brown, R. H., Cruikshank, D. P., Owen, T. C., Geballe, T. R., and DeBergh, C.: 1994, 'The Temperature of Nitrogen Ice on Pluto and its Implications for Flux Measurements', *Icarus* **112**, 513–527.

Tyler, G. L., Sweetnam, D. N., Anderson, J. D., Borutzki, S. E., Campbell, J. K., Eshleman, V. R., Gresh, D. L., Gurrola, E. M., Hinson, D. P., Kawashima, N., Kursinski, E. R., Levy, G. S., Lindal, G. F., Lyons, J. R., Marouf, E. A., Rosen, P. A. Simpson, R. A., and Wood, G. E.: 1989, 'Voyager Radio Science Observations of Neptune and Triton', *Science* **246**, 1466–1473.

Walker, A. R.: 1980, 'An Occultation by Charon', *Mon. Not. Roy. Astron. Soc.* **192**, 47–50.

Yelle, R. V. and Elliot, J. L.: 1997, 'Atmospheric Structure and Composition: Pluto and Charon', in S. A. Stern and D. J. Tholen (eds.), *Pluto and Charon*, University of Arizona Press, Tucson, AZ, pp. 347–390.

Yelle, R. V. and Lunine, J. I.: 1989, 'Evidence for a Molecule Heavier than Methane in the Atmosphere of Pluto', *Nature* **339**, 288–290.

Yelle, R. V., Lunine, J. I., Pollack, J. B., and Brown, R. H.: 1995, 'Lower Atmospheric Structure and Surface-Atmosphere Interactions on Triton', in D. P. Cruikshank (ed.), *Neptune and Triton*, University of Arizona Press, Tucson, pp. 1031–1105.

Young, E. F. and Binzel, R. P.: 1994, 'A New Determination of Radii and Limb Parameters for Pluto and Charon from Mutual Event Lightcurves', *Icarus* **108**, 219–224.

Young, L. A., Elliot, J. L., Tokunaga, A., de Bergh, C., and Owen, T.: 1997, 'Detection of Gaseous Methane on Pluto', *Icarus* **127**, 258–262.